INTERNATIONAL JOURNAL FOR NUMERICAL METHODS IN FLUIDS, VOL. 16, 953–966 (1993)

CALCULATION OF QUASI-THREE-DIMENSIONAL INCOMPRESSIBLE VISCOUS FLOWS BY THE FINITE ELEMENT METHOD

M. SEDLÁŘ

Pump Research Institute, Olomouc, Kosmonautů 6, 772 23 Olomouc, Czechoslovakia

SUMMARY

This paper discusses the calculation of quasi-three-dimensional incompressible viscous flow by FEM. The Reynolds-averaged Navier–Stokes equations are solved in curvilinear co-ordinates by the reduced integration and penalty method (RIP). Streamline upwind artificial viscosity (SUAV) and the Baldwin–Lomax algebraic model of turbulence are used. Time discretization is by the general implicit θ-method.

KEY WORDS Curvilinear co-ordinate system Incompressible viscous flow Finite elements Penalization and reduced integration Streamline upwind artificial viscosity Algebraic model of turbulence

INTRODUCTION

This paper presents a numerical modelling of the incompressible viscous flow by the finite element method (FEM), using a standard personal computer. The fully three-dimensional flow is approximated by the quasi-three-dimensional model of flow in two sets of stream surfaces, one extending in the circumferential direction, and the other in the radial direction.[1,2] The formulation of this problem is based on the theory presented by Girault and Raviart.[3] Penalization and reduced integration[4,5,6] are used to eliminate the pressure unknown from the system of equations to be solved. The quadratic triangular element satisfying some Oden[4] requirements is used. To obtain the wiggle-free solution and to eliminate any crosswind artificial diffusion, the mesh refinement and the streamline upwind artificial viscosity method are applied. (Artificial viscosity is added only in the flow direction.) This method is based on the approach of Thomasset,[7] Brooks and Hughes,[8] Gresho and Lee,[9] Kikuchi and Ushijima,[10] Maršík and Daněk,[11] etc. The Baldwin–Lomax algebraic model of turbulence as modified by Rodi and Srinivas[12] has been selected so that calculations could be realized on a standard personal computer.

FORMULATION OF STATIONARY PROBLEM

First, we formulate the problem of the stationary turbulent flow using curvilinear co-ordinates. Let q_1, q_2, q_3 be curvilinear orthogonal co-ordinates with the Lame coefficients $L_1 = L_1(q_2)$, $L_2 = L_2(q_1)$, $L_3 = L_3(q_1, q_2)$, $(q_1 q_2)$ be a computational stream surface with $q_3 = \text{constant}$ and $L_3 = \Delta(q_3)$ be the variable thickness of fluid layer over $(q_1 q_2)$. Moreover, suppose that the velocity $\mathbf{u} = (u_1, u_2, 0)$ is parallel to the computational stream surface, $\partial\mathbf{u}/\partial q_3 = \mathbf{0}$ and $\operatorname{div}(\mathbf{u}) = 0$.

Consider the dimensionless problem, that is, $\nu = Re^{-1}$. Let ν_e (effective viscosity) be a known function and $\mathbf{u}$ (velocity) and p (pressure) be unknown functions. Now the problem can be

0271–2091/93/110953–14$12.00

Received June 1992
Revised December 1992

formulated this way:

$$(\mathbf{u}\cdot\nabla)\mathbf{u}=\nabla\cdot(\nu_e\nabla\mathbf{u})+\nabla\cdot(\nu_e\nabla\mathbf{u})^*-\nabla p+\mathbf{f},\quad \text{in } \Omega, \tag{1}$$

$$\operatorname{div}(\mathbf{u})=0,\quad \text{in } \Omega, \tag{2}$$

$$\mathbf{u}|_{\Gamma_1}=\boldsymbol{\tau}\quad \text{(inflow and adherence boundary condition)}, \tag{3}$$

$$\nu_e\frac{\partial\mathbf{u}}{\partial n}-p\mathbf{n}|_{\Gamma_2}=\mathbf{0}\quad \text{(outflow boundary condition)}, \tag{4}$$

$$\mathbf{u}|_{\Gamma_3^1}=\mathbf{u}|_{\Gamma_3^2},\quad \left.\frac{\partial\mathbf{u}}{\partial n}\right|_{\Gamma_3^1}=-\left.\frac{\partial\mathbf{u}}{\partial n}\right|_{\Gamma_3^2},\quad p|_{\Gamma_3^1}=p|_{\Gamma_3^2}$$

$$\text{(periodic boundary condition)}. \tag{5}$$

Here $\Gamma_1\cup\Gamma_2\cup\Gamma_3=\Gamma$ is a boundary of a Lipschitz continuous bounded domain Ω, $\mathbf{n}|_{\Gamma_3^1}=-\mathbf{n}|_{\Gamma_3^2}$ and $f|_\Gamma$ is the restriction of a function f on Γ (see Figure 1).

Let us introduce the following function spaces:

$$Z=\{\mathbf{v}\in(W^{1,2}(\Omega))^2,\ \mathbf{v}|_{\Gamma_1}=\mathbf{0},\ \mathbf{v}|_{\Gamma_3^1}=\mathbf{v}|_{\Gamma_3^2}\}, \tag{6}$$

$$W=\{\mathbf{v}\in(W^{1,2}(\Omega))^2,\ \operatorname{div}(\mathbf{v})=0\}, \tag{7}$$

$$V=\{\mathbf{v}\in Z,\ \operatorname{div}(\mathbf{v})=0\}, \tag{8}$$

$$M=\{r\in L^2(\Omega)\}, \tag{9}$$

$$(M=\{r\in L^2(\Omega),\ (r,1)=0\}\ \text{when } \Gamma_2=\emptyset) \tag{9'}$$

and operators:

$$a(\mathbf{u},\mathbf{v})=(\nu_e\nabla\mathbf{u},\nabla\mathbf{v}), \tag{10}$$

$$b(\mathbf{w};\mathbf{u},\mathbf{v})=((\mathbf{w}\cdot\nabla)\mathbf{u},\mathbf{v}), \tag{11}$$

$$c(\mathbf{u},\mathbf{v})=(-\nabla\cdot(\nu_e\nabla\mathbf{u})^*,\mathbf{v}), \tag{12}$$

$$\langle 1,\mathbf{v}\rangle=(\mathbf{f},\mathbf{v}). \tag{13}$$

Here $(.\,,.)$ is the scalar product in $L^2(\Omega)$, the dot represents the scalar product in R^2, and $W^{k,p}(\Omega)$ is the usual Sobolev space. We suppose that $\boldsymbol{\tau}$ is a trace of some function $\mathbf{t}\in W$. Now we can formulate weakly the problem defined by equations (1)–(5), as follows:

$$\mathbf{u}-\mathbf{t}\in V,\quad p\in M, \tag{14}$$

$$a(\mathbf{u},\mathbf{v})+b(\mathbf{u};\mathbf{u},\mathbf{v})+c(\mathbf{u},\mathbf{v})-(p,\operatorname{div}(\mathbf{v}))=\langle l,\mathbf{v}\rangle,\quad \forall\mathbf{v}\in Z. \tag{15}$$

We define the finite-dimensional spaces $Z_h\subset Z$, $M_h\subset M$ for every h (h is a characteristic parameter of a mesh) and the space

$$V_h=\{\mathbf{v}_h\in Z_h,\ (q_h,\operatorname{div}(\mathbf{v}_h))=0,\quad \forall q_h\in M_h\}. \tag{16}$$

Now the problem defined by equations (14) and (15) can be formulated in the discrete form as

$$\mathbf{u}_h-\mathbf{t}_h\in V_h, \tag{17}$$

$$a(\mathbf{u}_h,\mathbf{v}_h)+b(\mathbf{u}_h;\mathbf{u}_h,\mathbf{v}_h)+c(\mathbf{u}_h,\mathbf{v}_h)=\langle l_h,\mathbf{v}_h\rangle,\quad \forall\mathbf{v}_h\in V_h, \tag{18}$$

or

$$\mathbf{u}_h-\mathbf{t}_h\in Z_h,\quad p_h\in M_h, \tag{19}$$

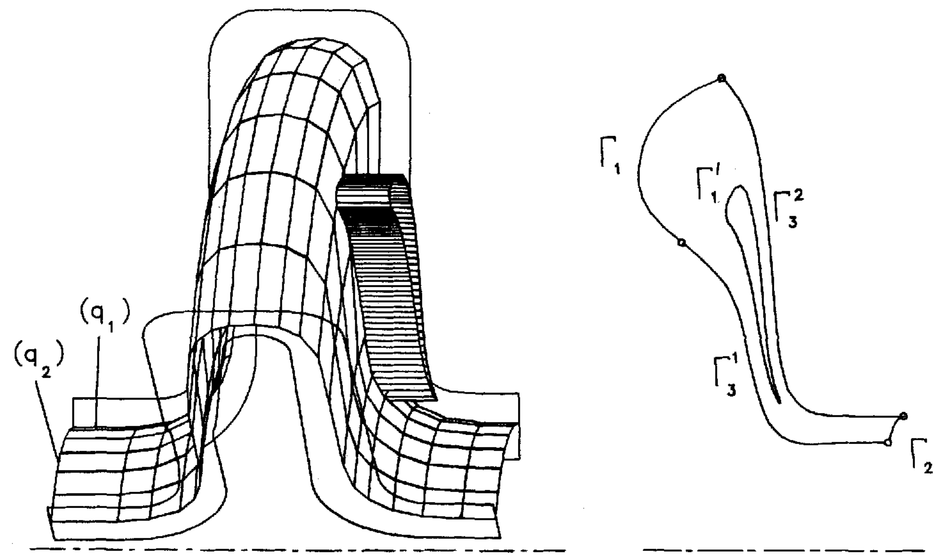

Figure 1. Co-ordinate lines and boundary description for cascade flow

$$a(\mathbf{u}_h, \mathbf{v}_h) + b(\mathbf{u}_h; \mathbf{u}_h, \mathbf{v}_h) + c(\mathbf{u}_h, \mathbf{v}_h) - (p_h, \operatorname{div}(\mathbf{v}_h)) = \langle l_h, \mathbf{v}_h \rangle, \quad \forall \mathbf{v}_h \in Z_h, \tag{20}$$

$$(\operatorname{div}(\mathbf{u}_h), q_h) = 0, \quad \forall q_h \in M_h. \tag{21}$$

PENALIZATION AND REDUCED INTEGRATION, FINITE ELEMENT DEFINITION

To eliminate the pressure from the system of equations, penalization is used. This is a regularization of the problem defined by equations (19)–(21) by means of

$$p_{\varepsilon, h} = -\frac{1}{\varepsilon} \rho_h(\operatorname{div}(\mathbf{u}_{\varepsilon, h})), \tag{22}$$

ρ_h being the orthogonal projection operator in $L^2(\Omega)$ onto M_h. Now the formulation has the form

$$\mathbf{u}_{\varepsilon, h} - \mathbf{t}_h \in Z_h, \tag{23}$$

$$a(\mathbf{u}_{\varepsilon, h}, \mathbf{v}_h) + b(\mathbf{u}_{\varepsilon, h}; \mathbf{u}_{\varepsilon, h}, \mathbf{v}_h) + c(\mathbf{u}_{\varepsilon, h}, \mathbf{v}_h) + \frac{1}{\varepsilon} (\rho_h(\operatorname{div}(\mathbf{u}_{\varepsilon, h})), \rho_h(\operatorname{div}(\mathbf{v}_h))) = \langle l, \mathbf{v}_h \rangle, \quad \forall \mathbf{v}_h \in Z_h. \tag{24}$$

The problem of the selection of parameter ε is described for the laminar case in Reference 6. In the case of turbulent flow, the situation is rather complicated and parameter ε is corrected during iteration.

The term $(\rho_h(\operatorname{div}(\mathbf{u}_{\varepsilon, h})), \rho_h(\operatorname{div}(\mathbf{v}_h)))$ is calculated by means of the reduced integration

$$(\rho_h(\operatorname{div}(\mathbf{u}_{\varepsilon, h})), \rho_h(\operatorname{div}(\mathbf{v}_h))) = I(\operatorname{div}(\mathbf{u}_{\varepsilon, h}) \operatorname{div}(\mathbf{v}_h)). \tag{25}$$

Here I is an integral calculated by a quadrature rule of order lower than the quadrature rule for the other members of equation (24).

As a finite element, the quadratic triangle is selected. The degrees of freedom are the velocities at the vertices and mid-side nodes. This element is suboptimal for the pure planar problem (it is of the same order of accuracy as the P_1 non-conforming triangle), but should be preferred in the case of curvilinear co-ordinates. Here P_k is the space of all polynomials of degree less than or equal to k (integer k). The quadrature rule, exact for P_3, with quadrature points in the vertices and barycentre is used for full integration;[13] the three-point rule with quadrature points in the mid-side nodes and the following formula

$$I(\operatorname{div}(\mathbf{u}_{\varepsilon,h})\operatorname{div}(\mathbf{v}_h))=\sum_K \frac{1}{\operatorname{meas}(K)}\int_K \operatorname{div}(\mathbf{u}_{\varepsilon,h})\,\mathrm{d}K \int_K \operatorname{div}(\mathbf{v}_h)\,\mathrm{d}K \tag{26}$$

are used for reduced integration[6] (here K is a finite element).

LINEARIZATION, UPWINDING

The non-linear problem defined by equation (24) can be linearized by successive approximation (which appears more robust than the Newton method) and then the following under-relaxation is used:

$$a(\mathbf{u}^n_{\varepsilon,h},\mathbf{v}_h)+b(\mathbf{w}^{n-1}_{\varepsilon,h};\mathbf{u}^n_{\varepsilon,h},\mathbf{v}_h)+c(\mathbf{u}^n_{\varepsilon,h},\mathbf{v}_h)+\frac{1}{\varepsilon}(\rho_h(\operatorname{div}(\mathbf{u}^n_{\varepsilon,h})),\rho_h(\operatorname{div}(\mathbf{v}_h)))=\langle l,\mathbf{v}_h\rangle,$$

$$\mathbf{w}^{n-1}_{\varepsilon,h}=\kappa\mathbf{u}^{n-1}_{\varepsilon,h}+(1-\kappa)\mathbf{u}^{n-2}_{\varepsilon,h}. \tag{27}$$

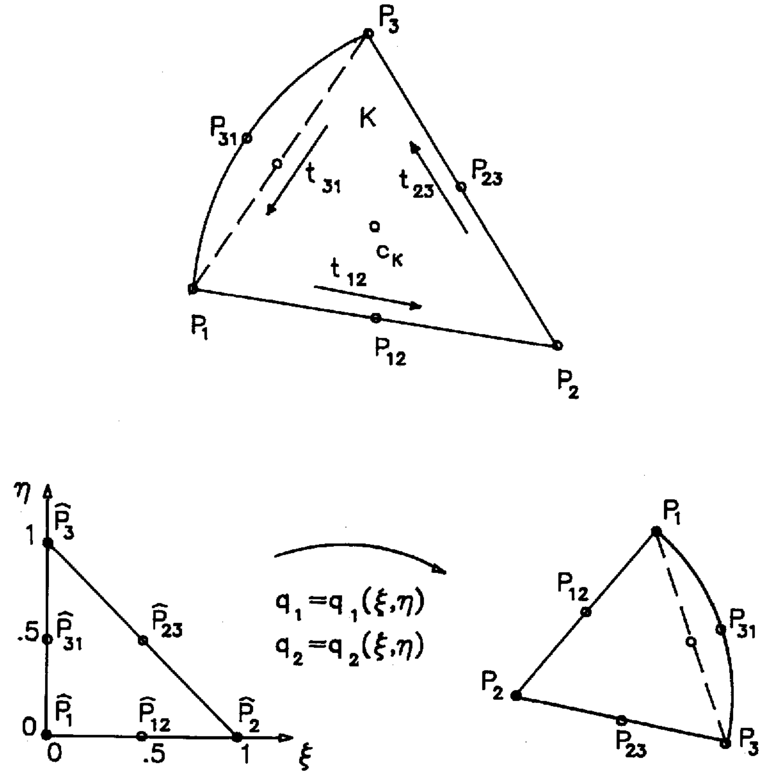

Figure 2. Finite element description

The upwinding method follows from the artificial viscosity method,[10,6] but now the artificial viscosity operator is constructed so as to operate in the flow direction only and to eliminate any crosswind artificial diffusion. The streamline-upwind formulation follows from References 7 and 8. Consider the equation

$$\frac{\partial \varphi}{\partial t}+(\mathbf{u}\cdot\nabla)\varphi=\nabla\cdot(\nu_e\nabla\varphi)+f$$

in curvilinear co-ordinates q_1, q_2, q_3 and choose the scalar artificial viscosity on a finite element K (Figure 2) as follows:

$$\nu_A=\begin{cases}\nu_e(c_K)\gamma\alpha/2 & \text{in the steady case,}\\ \nu_e(c_K)\gamma\alpha/\sqrt{15} & \text{in the transient case,}\end{cases}$$

$$\gamma=\frac{1}{\nu_e(c_K)}\max_{i\neq j}\left\{\|P_i-P_j\|\cdot\max_{\{P_i,P_j,P_{ij},c_K\}}|\mathbf{u}\cdot\mathbf{t}_{ij}|/2\right\},$$

$$\alpha=\coth\frac{\gamma}{2}-\frac{2}{\gamma}. \tag{28}$$

Here $\|\ \|$ is the norm in R^2, $\mathbf{t}_{ij}$ is the unit vector in the direction P_iP_j, and c_K is the barycentre of the element K. Now the artificial viscosity operator supplements the term $\nabla\cdot(\nu_e\nabla\varphi)$ on the finite element K with the term

$$(\nu_A/\|\mathbf{u}(c_K)\|^2)(\mathbf{u}(c_K)\cdot\nabla)^2\varphi. \tag{29}$$

TURBULENCE MODEL

Because calculations were made on a personal computer, great attention is devoted to the choice of a turbulence model. Both the algebraic models and the k–ε model have been considered. According to the literature,[12] algebraic models of turbulence are more robust and severally economical; moreover, the k–ε model shows no clear overall advantage. (For attached flow both models produce fairly good results, but in large separation regions neither of the models agrees sufficiently with the experimental results. Using the Baldwin–Lomax model, the predicted separation is usually too small, and the k–ε model tends to overpredict.)

From algebraic models of turbulence, modifications of the Rostand model and the Baldwin–Lomax model have been tested; the Baldwin–Lomax turbulence model in the modification presented in Reference 12 appears to be the most suitable.

TIME DISCRETIZATION

Analogous to the stationary problem, we now consider the following time-dependent problem:

$$\frac{\partial \mathbf{u}}{\partial t}+(\mathbf{u}\cdot\nabla)\mathbf{u}=\nabla\cdot(\nu_e\nabla\mathbf{u})+\nabla\cdot(\nu_e\nabla\mathbf{u})^*-\nabla p+\mathbf{f},\quad \text{in } \Omega\times \mathrm{R}^+, \tag{30}$$

$$\operatorname{div}(\mathbf{u})=0,\quad \text{in } \Omega\times\mathrm{R}^+, \tag{31}$$

$$\mathbf{u}|_{\Gamma_1\times\mathrm{R}^+}=\boldsymbol{\tau}, \tag{32}$$

$$\nu_e\frac{\partial \mathbf{u}}{\partial n}-p\mathbf{n}|_{\Gamma_2\times\mathrm{R}^+}=\mathbf{0}, \tag{33}$$

$$\mathbf{u}|_{\Gamma_3^1\times R^+}=\mathbf{u}|_{\Gamma_3^2\times R^+},\quad \frac{\partial \mathbf{u}}{\partial n}\bigg|_{\Gamma_3^1\times R^+}=-\frac{\partial \mathbf{u}}{\partial n}\bigg|_{\Gamma_3^2\times R^+},\quad p|_{\Gamma_3^1\times R^+}=p|_{\Gamma_3^2\times R^+}, \tag{34}$$

$$\mathbf{u}(t=0)=\mathbf{u}_0,\quad \text{in } \Omega. \tag{35}$$

Let us define the function space

$$H=\{\mathbf{v}\in(L^2(\Omega))^2,\quad \mathrm{div}(\mathbf{v})=0,\quad \mathbf{v}\cdot\mathbf{n}|_{\Gamma_1}=0\}. \tag{36}$$

Now the problem can be formulated as follows:

$$\mathbf{u}_\varepsilon-\mathbf{t}\in L^2(0,T;Z)\cap L^\infty(0,T;H),\quad \mathbf{u}_\varepsilon(t=0)=\mathbf{u}_0, \tag{37}$$

$$\left(\frac{\partial \mathbf{u}_\varepsilon}{\partial t},\mathbf{v}\right)+a(\mathbf{u}_\varepsilon,\mathbf{v})+b(\mathbf{u}_\varepsilon;\mathbf{u}_\varepsilon,\mathbf{v})+c(\mathbf{u}_\varepsilon,\mathbf{v})+\frac{1}{\varepsilon}(\rho(\mathrm{div}(\mathbf{u}_\varepsilon)),\rho(\mathrm{div}(\mathbf{v})))=\langle l,\mathbf{v}\rangle$$

$$\forall \mathbf{v}\in Z,\quad \text{in } D'(0,T). \tag{38}$$

Here $L^p(0,T;Z)$ is the abstract space of the vector-valued functions,[3] $D(0,T)$ is the space of functions infinitely differentiable and with compact support on $(0,T)$, and $D'(0,T)$ is the dual space of $D(0,T)$.

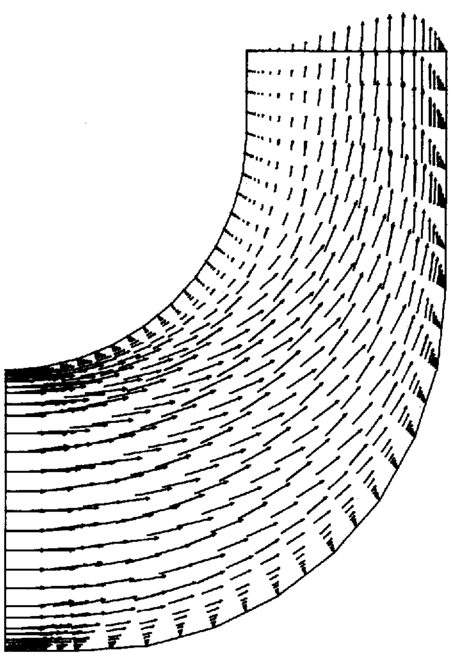

Figure 3. Meridional flow in the impeller of a centrifugal pump. Laminar case ($Re=10^3$)

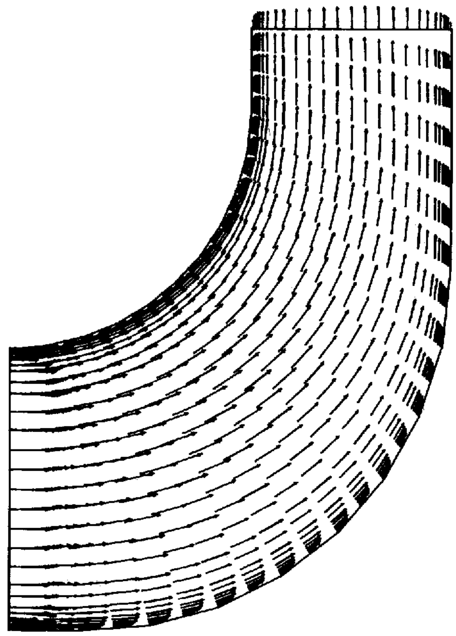

Figure 4. Meridional flow in the impeller of a centrifugal pump. Turbulent case ($Re=10^5$)

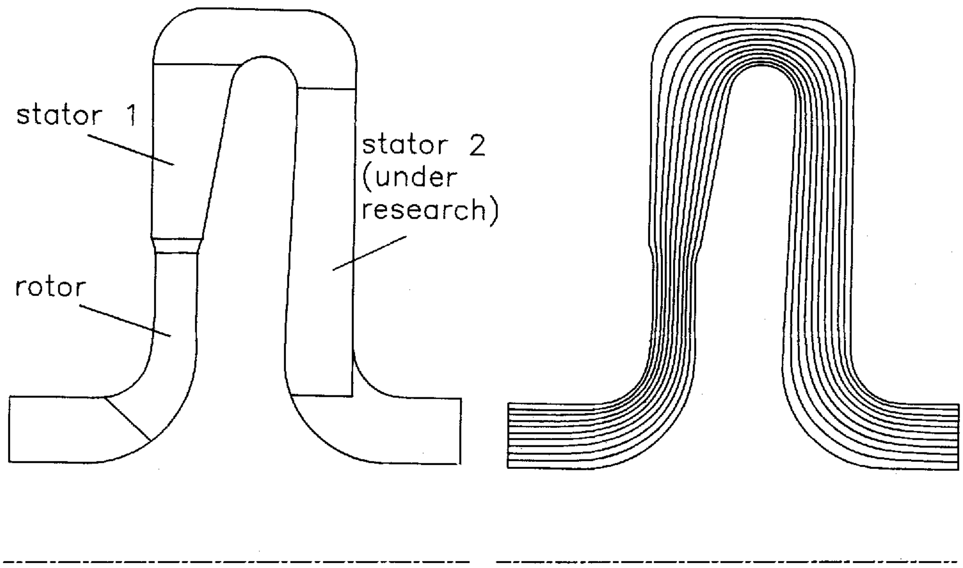

Figure 5. Streamlines in a stage of a centrifugal pump

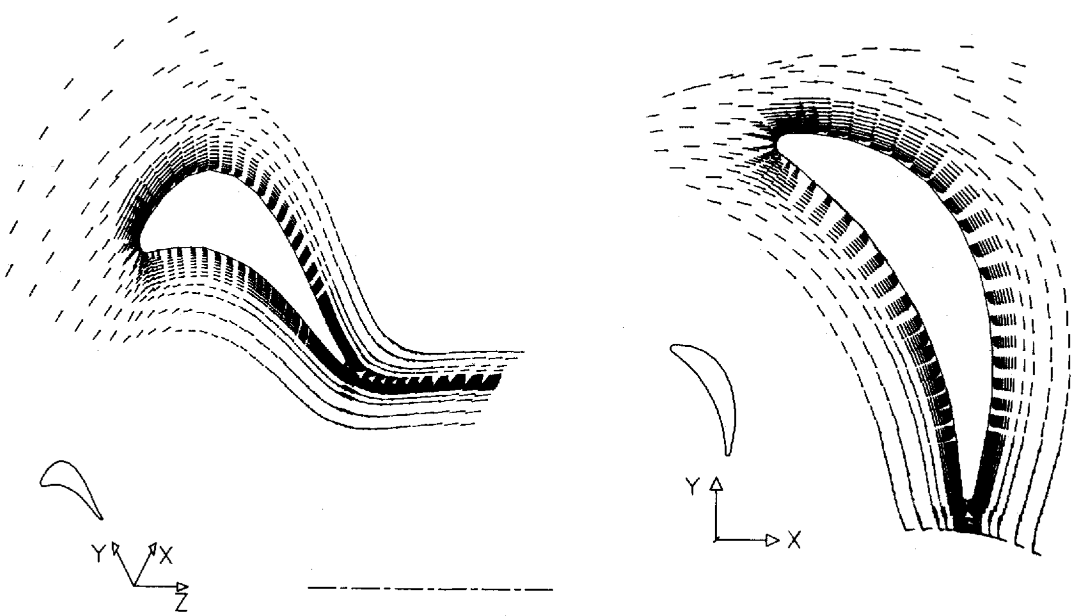

Figure 6. Flow past a stator blade of a centrifugal pump ($Re = 2 \times 10^5$)

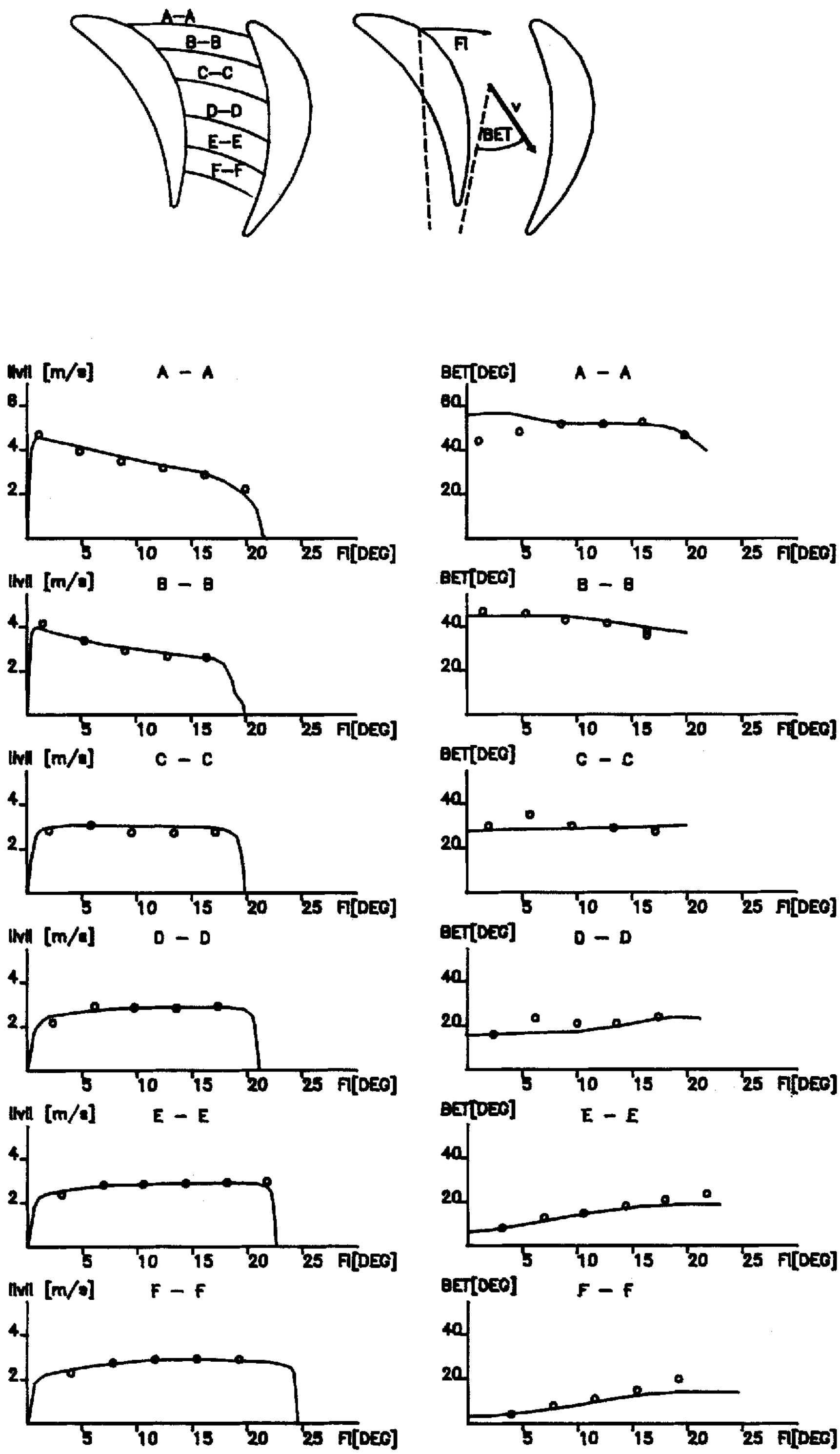

Figure 7. Comparison of the calculation with the LDA experiment: —— calculation; ○ experiment

Consider the general θ-method of time discretization:[3]

$$y' + f(t, y) = 0,$$

$$\frac{1}{\Delta t}(y^n - y^{n-1}) = -\theta f(t_n, y^n) - (1-\theta) f(t_{n-1}, y^{n-1}).$$

This is the so-called fully implicit scheme for $\theta = 1$ (of the first order and strongly A-stable) and the so-called trapezoidal rule for $\theta = 0{\cdot}5$ (of the second order and A-stable).

Let us define an operator

$$a_0(\mathbf{u}, \mathbf{v}) = \frac{1}{\Delta t}(\mathbf{u}, \mathbf{v}). \tag{39}$$

Now the problem can be formulated in the discrete form

$$a_0(\mathbf{u}^n_{\varepsilon,h}, \mathbf{v}_h) + \theta \left[a(\mathbf{u}^n_{\varepsilon,h}, \mathbf{v}_h) + b(\mathbf{w}^{n-1}_{\varepsilon,h}; \mathbf{u}^n_{\varepsilon,h}, \mathbf{v}_h) + c(\mathbf{u}^n_{\varepsilon,h}, \mathbf{v}_h) + \frac{1}{\varepsilon}(\rho_h(\operatorname{div}(\mathbf{u}^n_{\varepsilon,h})), \rho_h(\operatorname{div}(\mathbf{v}_h))) - \langle l^n, \mathbf{v}_h \rangle \right]$$

$$= a_0(\mathbf{u}^{n-1}_{\varepsilon,h}, \mathbf{v}_h) + (\theta - 1) \left[a(\mathbf{u}^{n-1}_{\varepsilon,h}, \mathbf{v}_h) + b(\mathbf{w}^{n-1}_{\varepsilon,h}; \mathbf{u}^{n-1}_{\varepsilon,h}, \mathbf{v}_h) + c(\mathbf{u}^{n-1}_{\varepsilon,h}, \mathbf{v}_h) \right.$$

$$\left. + \frac{1}{\varepsilon}(\rho_h(\operatorname{div}(\mathbf{u}^{n-1}_{\varepsilon,h})), \rho_h(\operatorname{div}(\mathbf{v}_h))) - \langle l^{n-1}, \mathbf{v}_h \rangle \right],$$

$$\mathbf{w}^{n-1}_{\varepsilon,h} = \kappa \mathbf{u}^{n-1}_{\varepsilon,h} + (1-\kappa)\mathbf{u}^{n-2}_{\varepsilon,h}. \tag{40}$$

When $\theta = 1$, it suffices to take $\kappa = 1$; when $\theta = 0{\cdot}5$, we must take $\kappa = 1{\cdot}5$, so as to obtain the second-order scheme.

SOME NUMERICAL RESULTS

Many numerical tests were carried out[6] to verify the numerical algorithms presented, and the results agreed well with the literature. Some calculations and comparisons with experiments are presented in this paper.

The meridional flow calculation in the centrifugal pump is presented in Figures 3 and 4. Shown in Figure 3 is the velocity field of laminar flow ($Re = 10^3$); in Figure 4, the velocity field of turbulent flow ($Re = 10^5$). (The Reynolds number is related to the inlet diameter and inlet velocity.)

The flow in the stator of a radial centrifugal pump is presented in Figures 5–7. Figure 6 shows the flow calculation in the central axisymmetric stream surface S_1 (the projection of which is the central streamline of meridional flow—see Figure 5). The fluid layer thickness over this stream surface S_1 varies according to the distance between the neighbouring streamlines of the meridional solution. (The Reynolds number $Re = 2 \times 10^5$ is related to the profile chord and inlet velocity.) Calculations and experimental data (LDA experiments[14] conducted in the Pump Research Institute, Olomouc) are compared in Figure 7.

The flow in the ŠKODA-ETALON SE1050 turbine cascade (experiments conducted in the Institute of Thermomechanics, Czechoslovak Academy of Sciences[15]) is presented in Figures 8–10. Figure 8 shows the velocity field of the tubrulent flow. (The Reynolds number

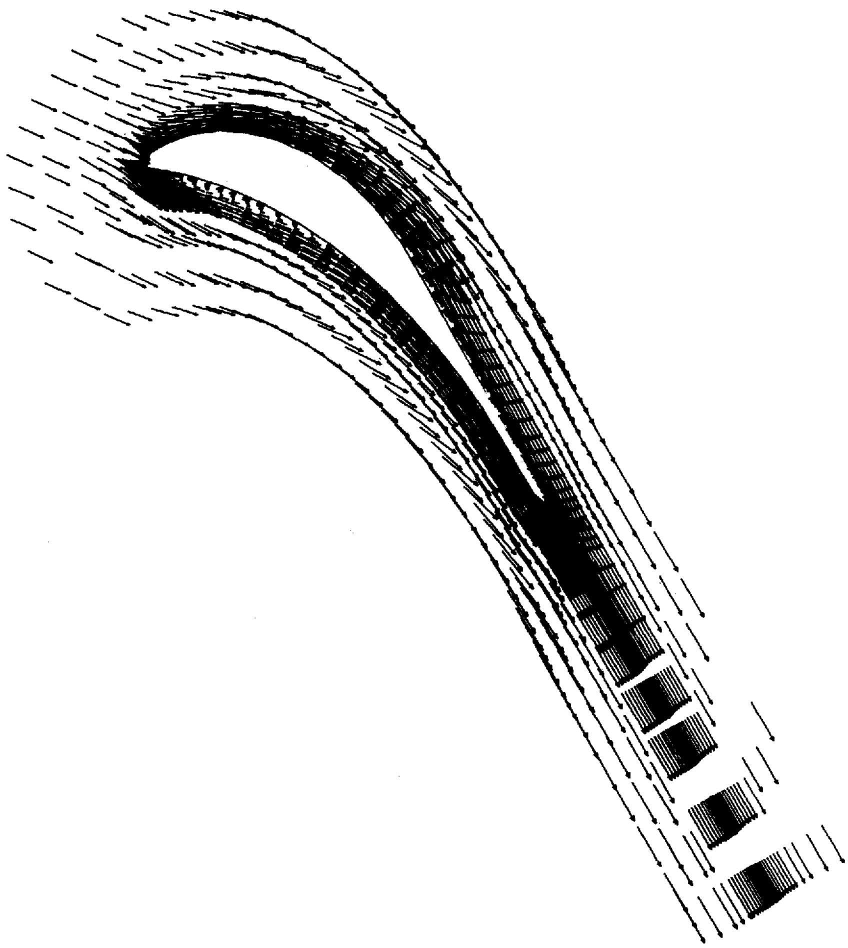

Figure 8. Flow past the ŠKODA-ETALON SE1050 turbine blade ($Re = 1{\cdot}1 \times 10^6$)

relating to the profile chord and the outlet isentropic Mach number $Re_{is} = 1{\cdot}1 \times 10^6$, the outlet isentropic Mach number $M_{2is} = 0{\cdot}511$, and the incidence angle $i = -40°$.) Figure 9 shows the constant-pressure lines resulting from the calculation relative to an interferogram. The distribution of pressure along the blade surface is shown in Figure 10. We have presumed that differences between incompressible and compressible flows are negligible for Mach numbers up to 0·5, and that the flow is adiabatic, to allow the evaluation of the interferogram and a comparison of the calculations with the experimental data.

All the above calculations were carried out as a steady-state case. Figure 11 shows the time-dependent calculation of flow past a circular cylinder and the development of the Karman vortex street. (The Reynolds number $Re = 10^2$ is based on the inlet velocity and the cylinder diameter.) The resulting Strouhal number $Sh = 0{\cdot}162$.

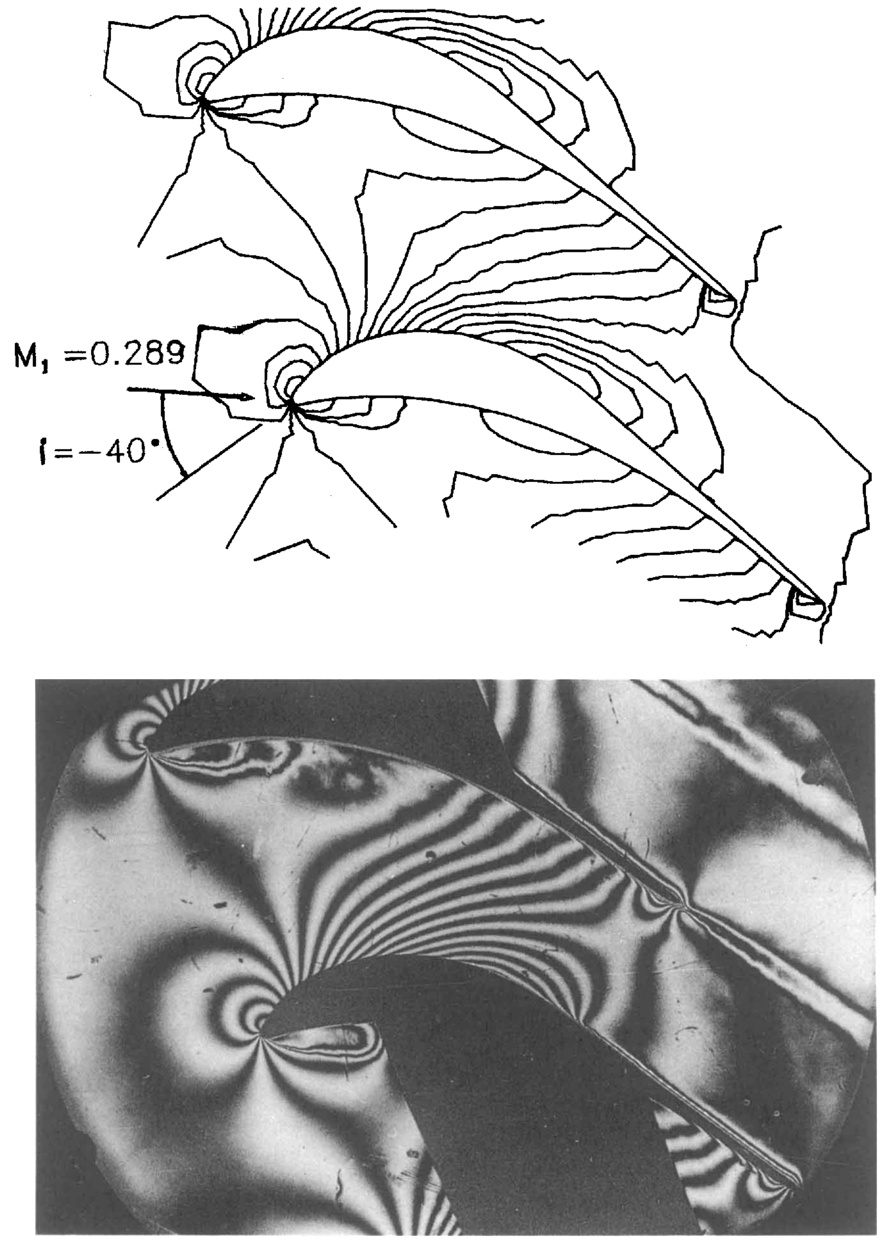

Figure 9. Comparison of constant-pressure lines with an interferogram

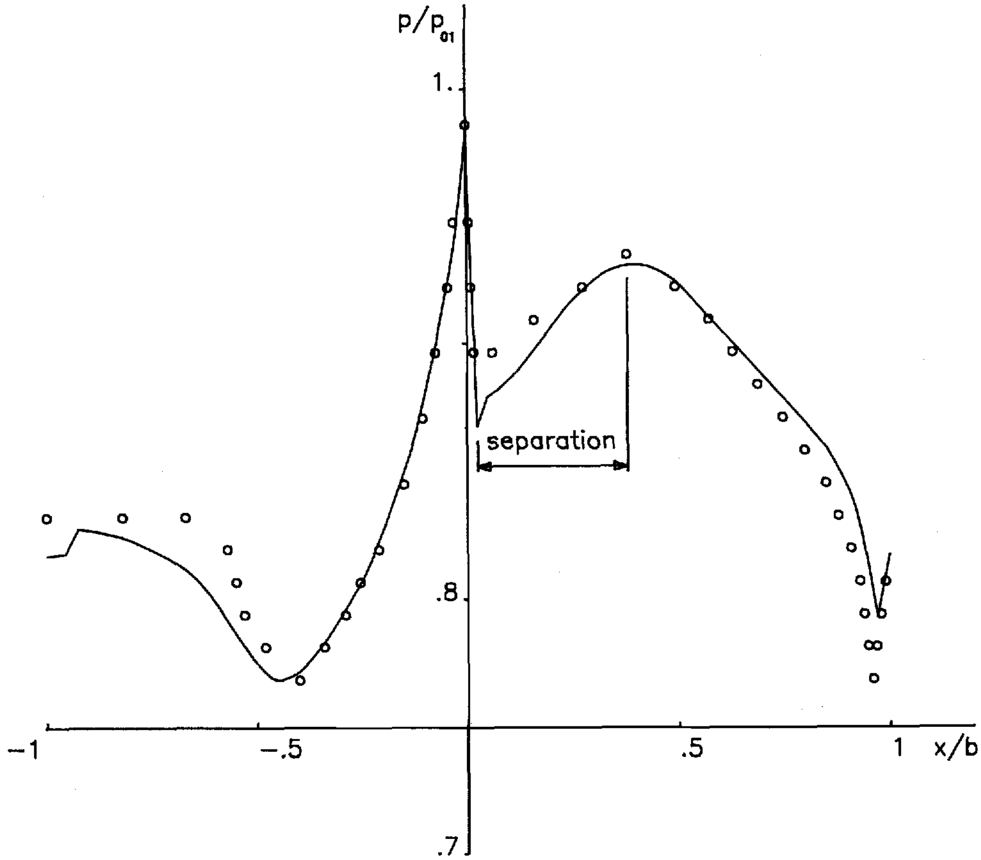

Figure 10. Distribution of pressure along the blade surface (p_{01} is the total pressure in the inlet plane, b is the chord length): —— calculation; ○ experiment

CONCLUSIONS

Numerical results presented were obtained from overly coarse grids because a standard PC-AT was used for the calculations. (Blade-to-blade computational times were over 30 h on a 286/16 MHz PC and about 2·5 h on a 486/33 MHz PC; meridional calculations took about half of these times.) In spite of these limitations, qualitatively, the results agree well with the experimental data, and we are encouraged to continue this work and develop a more general quasi-three-dimensional attitude with full accounting for the interaction between the S_1 and S_2 solutions.

ACKNOWLEDGEMENTS

This work was carried out in partial fulfillment of Ph.D. studies in the Institute of Thermomechanics, Czechoslovak Academy of Sciences, with help from Ing. F. Maršík, DrSc., Ing. P. Šafařík, CSc. and Ing. J. Příhoda, CSc. All calculations were made on a standard PC-AT with coprocessor in the Pump Research Institute, Olomouc, Czechoslovakia.

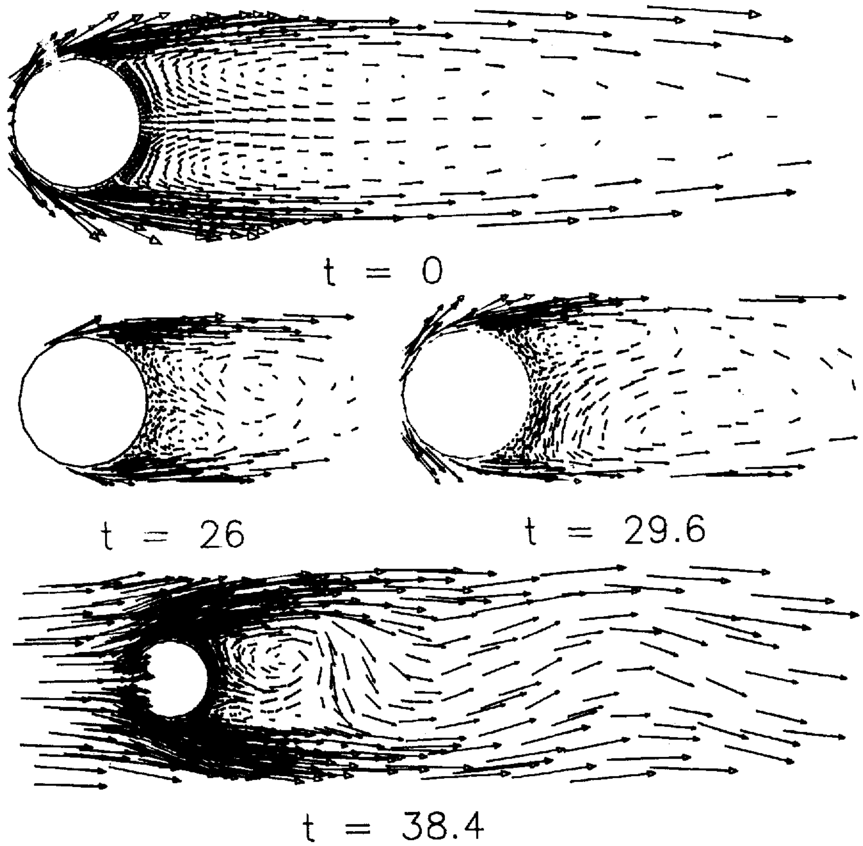

Figure 11. Flow past a circular cylinder. Karman vortex street ($Re = 10^2$)

APPENDIX: NOMENCLATURE

Ω	bounded domain with Lipschitz continuous boundary
Γ	boundary of Ω
$D(\Omega)$	space of functions infinitely differentiable and with compact support on Ω
$W^{k,p}(\Omega)$	Sobolev space
$L^p(0, T; V)$	abstract space of vector-valued functions
$\Vert\ \Vert$	norm on R^2
$\cdot$	scalar product of R^2
V'	dual space of V
$(.,.)$	scalar product of $L^2(\Omega)$
$\langle .,. \rangle$	duality
meas(K)	measure of the set K
$v\vert_K$	restriction of the function v on the set K
h	characteristic parameter of a mesh
T_h	triangulation of a domain
P_k	space of all polynomials of degree less than or equal to k in two variables
q_1, q_2, q_3	curvilinear orthogonal co-ordinates

L_1, L_2, L_3	Lame coefficients
(q_3)	co-ordinate line (q_1 = constant, q_2 = constant)
$(q_1 q_2)$	computational co-ordinate surface (q_3 = constant)
$\Delta(q_3)$	variable thickness of fluid layer
$\mathbf{n}$	unit outward normal
$\frac{\partial}{\partial n}$	normal derivative
$\mathbf{u}$	velocity
p	static pressure
p_0	total pressure
p_{01}	total pressure at the inlet plane
ν	kinematic viscosity
ν_e	effective viscosity, $\nu_e = \nu + \nu_t$
ν_t	turbulent viscosity
Re	Reynolds number
M	Mach number
b	chord length
i	incidence angle

REFERENCES

1. C. H. Wu, 'A general theory of three-dimensional flow in subsonic and supersonic turbomachines on axial-, radial-, and mixed-flow types', *NACA TN 2604*, 1952.
2. M. Bajorek and M. Sedlář, 'Model of fluid flow in the variable thickness of a fluid layer and its solution by the finite element method', *Stroj. čas.*, **4**, 281–297 (1992).
3. V. Girault and P. A. Raviart, *Finite Element Approximation of the Navier–Stokes Equations*, Lecture Notes in Mathematics, Springer, Berlin, 1979.
4. J. T. Oden, 'RIP-methods for Stokesian flows', *Finite Elements Fluids*, **4**, 305–318 (1982).
5. M. Bercovier and M. Engelmann, 'A finite element for the numerical solution of viscous incompressible flows', *J. Comput. Phys.*, **30**, 181–201 (1979).
6. M. Sedlář, 'Solution of the Navier–Stokes equations for incompressible steady flow by the penalty and reduced integration method', *ČPA*, **1**, 12–17 (1990).
7. F. Thomasset, *Implementation of Finite Element Methods for Navier–Stokes Equations*, Springer series Comput. Physics, Springer, Berlin, 1981.
8. A. N. Brooks and T. J. R. Hughes, 'Streamline upwind/Petrov–Galerkin formulations for convection-dominated flows with particular emphasis on the incompressible Navier–Stokes equations', *Comput. methods appl. mech. eng.*, **32**, 199–259 (1982).
9. P. M. Gresho and R. L. Lee, 'Don't suppress the wiggles—they're telling you something!', *Comput. Fluids*, **9**, 223–253 (1981).
10. F. Kikuchi and T. Ushijima, 'Theoretical analysis of some finite element methods for convective diffusion equations', *Finite Elements Fluids*, **4**, 67–87 (1982).
11. F. Maršík and V. Daněk, 'The role of dissipation in hyperbolic problems solved by FEM', in K. Kozel (ed.), *Mathematical Modelling in Engineering*, UK Praha, 1991, pp. 54–59.
12. W. Rodi and K. Srinivas, 'Computation of flow and losses in transonic turbine cascades', *Z. Flugwiss, Weltraumforsch*, **13**, 101–119 (1989).
13. P. G. Ciarlet and P. A. Raviart, 'The combined effect of curved boundaries and numerical integration in isoparametric FEM', in A. K. Aziz (ed.), *The Mathematical Foundations of the FEM with Applications to PDE*, Academic Press, New York, 1972.
14. J. Šoukal, 'Viscous flow in stator of a radial centrifugal pump', *Ph.D. Thesis*, Pump Research Institute, Olomouc, 1991.
15. M. Šťastný and P. Šafařík, 'Experimental analysis data on the transonic flow past a plane turbine cascade', *ASME Paper 90-GT-313*, 1990.